ELSEVIER

Journal of Atmospheric and Solar-Terrestrial Physics 70 (2008) 219–225

Journal of ATMOSPHERIC AND SOLAR-TERRESTRIAL PHYSICS

www.elsevier.com/locate/jastp

Solar cycle variations of solar wind dynamics and structures

J.D. Richardson[a,b,*], J.C. Kasper[a]

[a]*Kavli Center for Astrophysics and Space Research, Massachusetts Institute of Technology, Cambridge, MA 02139, USA*
[b]*State Key Laboratory of Space Weather, Center for Space Science and Applied Research, Chinese Academy of Sciences, P.O. Box 8701, Beijing 100080, China*

Accepted 27 August 2007
Available online 2 October 2007

Abstract

This paper reviews solar cycle variations in the heliosphere. We show that some solar cycle changes, such as the correlation between speed and density, result from the evolution of the solar structure from dipolar with strong latitudinal gradients at solar minimum to a disordered field with little latitudinal variation at solar maximum. Other changes, such as the variation of the solar wind dynamic pressure, occur at all heliolatitudes independent of the solar wind structure. The solar cycle dependence of interplanetary coronal mass ejections (ICMEs) results in changes in the solar wind structure in the outer heliosphere, with large merged interaction regions (MIRs) driven by ICMEs near solar maximum. The helium/proton (He/H) ratio also changes over the solar cycle and suggests that the slow solar wind has two sources, one poor in He and the other with larger He/H ratios.

Keywords: ICMEs; Solar wind; Heliosphere; Solar cycle

1. Introduction

The solar wind was first measured in 1959 (Gringauz, 1961) and the first systematic observations were made in 1962 (Neugebauer and Snyder, 1966). Solar cycle changes in the solar wind were reviewed by Neugebauer (1975) and Gazis (1996). Many aspects of the solar wind change over a solar cycle, including the speed, the density, the dynamic pressure, the latitudinal structure, the composition, and the temperature. As new regions of the solar system have been explored, such as high-latitudes with Ulysses and large distances with the Pioneers and Voyagers, we have found new evidence of solar cycle effects. Better instrumentation has provided a clearer picture of solar cycle variations near Earth. This paper reviews and updates recent results on the solar cycle variation of solar wind and solar wind structure.

2. Solar cycle dependence of the solar wind

The basic configuration of the magnetic field and solar wind change over a solar cycle is illustrated in Fig. 1. At solar minimum, the magnetic field is dipolar and the average solar wind magnetic field magnitude at 1 AU is small (Burlaga et al., 2002). The solar poles are covered by coronal holes which eject high-speed, >700 km/s solar wind whereas the

*Corresponding author. Kavli Center for Astrophysics and Space Research, Massachusetts Institute of Technology, Cambridge, MA 02139, USA. Tel.: +1 617 253 6112; fax: +1 617 253 0861.
E-mail address: jdr@space.mit.edu (J.D. Richardson).

1364-6826/$ - see front matter © 2007 Elsevier Ltd. All rights reserved.
doi:10.1016/j.jastp.2007.08.039

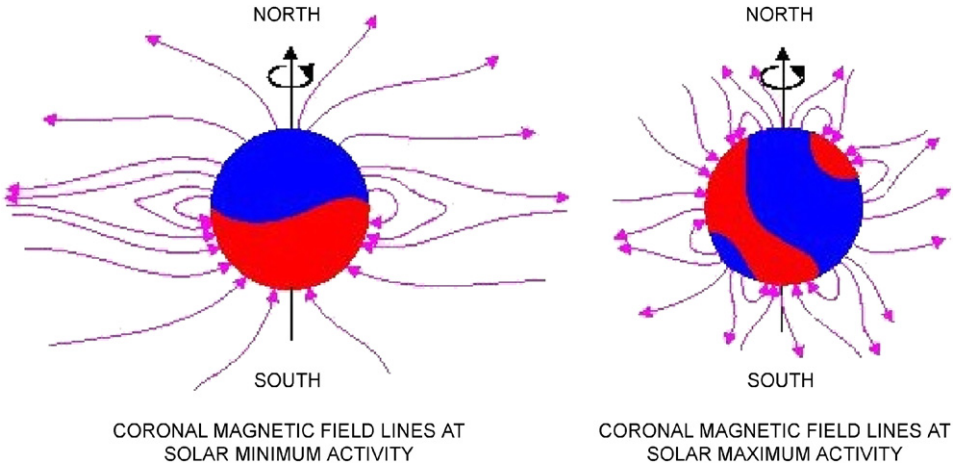

Fig. 1. A schematic diagram showing the change in the solar magnetic field configuration from dipolar with a small current sheet tilt at solar minimum to disordered at solar maximum. Adapted from http://www.sp.ph.ic.ac.uk/~forsyth/reversal.

streamer belt and current sheet are near the equator and are a source of low-speed, 400 km/s solar wind (see Gazis, 1996). Few interplanetary coronal mass ejections (ICMEs) occur near solar minimum, so few shocks form (see Cane and Richardson, 2003), and the average helium abundance (averaged over all solar wind conditions) is low, 1–2% (Aellig et al., 2001). At solar maximum, the magnetic field is disordered. The polar coronal holes are less prevalent and the solar wind is dominated by slow solar wind at all heliolatitudes (McComas et al., 2000). ICMEs are frequent, making up 15% of the solar wind at Earth (Gosling et al., 1992) and up to 40% in the outer heliosphere (Richardson et al., 2006). ICMEs are the source of most of the fast wind observed and these ICMEs often have leading shocks. The average helium density is high, averaging 5% (Aellig et al., 2001).

Fig. 2 shows the variation of the correlation between solar wind speed and density, 50-day running averages of the dynamic pressures observed by IMP 8 and Voyager 2 (normalized to 1 AU), and the monthly sunspot number. The correlations of daily averages of the solar wind speed and density observed by IMP 8 from launch in 1973 through 2006 are shown in the top panel. The speed and density are anti-correlated near solar minimum, since the solar wind at Earth alternates between slow, dense streamer flow and hot, tenuous coronal hole flow. At solar maximum the anti-correlation is much weaker, since the high-speed, tenuous coronal hole flow is not present and ICMEs, which provide most of the solar maximum fast flow, have densities similar to the ambient solar wind.

The solar wind dynamic pressure, the mass density times the speed squared, also changes over the solar cycle. The pressure profile shown in Fig. 2 has a minimum near the solar maxima in 1979, 1990, and 2000; in 1979 and 1990 the pressure minima were followed by a rapid factor of two increase in pressure, then a slow decline in pressure until the next solar maximum. In the current solar cycle, the increase in the dynamic pressure has been smaller than in previous cycles. When only ecliptic solar wind data were available, it was not known whether the observed changes in dynamic pressure were due to solar cycle variations at low-latitudes or occurred at all latitudes. This distinction was important, since the solar wind pressure changes drive changes in the size of the heliosphere and the locations of the termination shock and heliopause boundaries. Different pressure profiles with time at different latitudes would have led to changes in the shape of the heliosphere over the solar cycle. When Ulysses was launched and went to high-latitudes, near solar minimum it observed very different solar wind than observed by spacecraft at low-latitudes. Comparison of the speeds and densities from IMP 8, Ulysses, and V2 often showed very different structure, but the pressure profiles looked very similar (Richardson and Wang, 1999). Thus the dynamic pressure change occurs at all latitudes so pressure changes at the termination shock are symmetric.

ICMEs drive many changes in the solar wind, especially as the solar wind moves to large distances. As large ICMEs move outward, a leading shock forms as the ICME pushes against the ambient solar

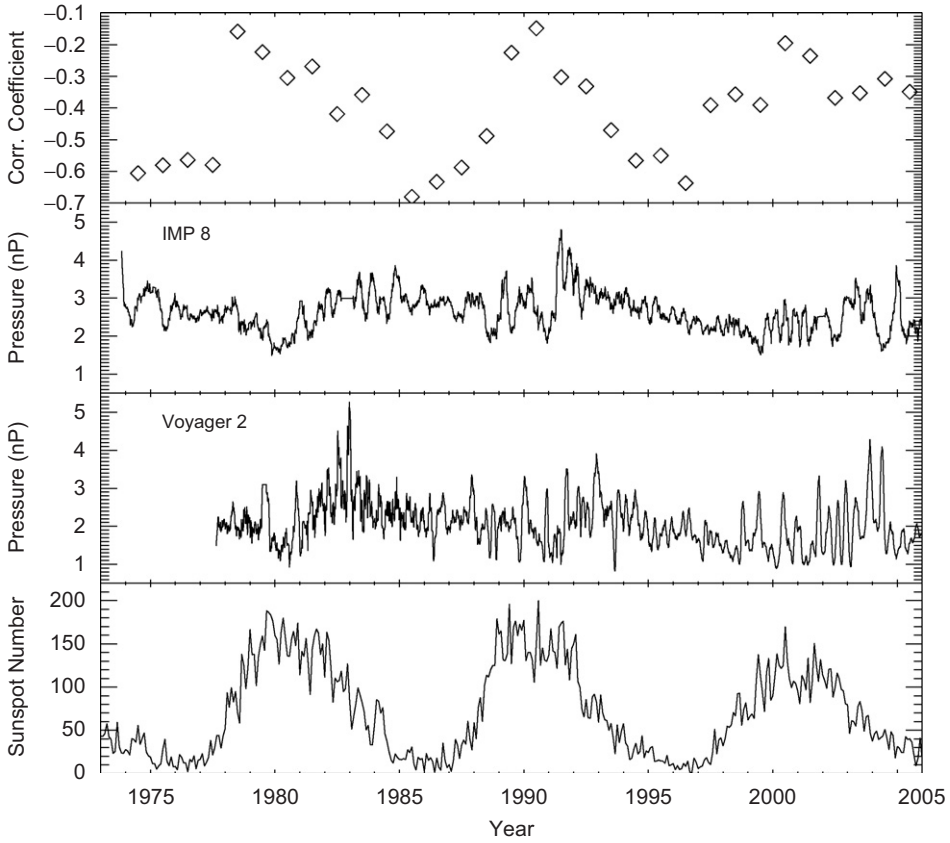

Fig. 2. The variation of the correlation between IMP 8 daily averages of speed and density, 50-day averages of the solar wind dynamic pressure observed by IMP 8, 50-day averages of the solar wind dynamic pressure observed by Voyager 2 normalized to 1 AU, and the monthly average sunspot number.

wind in front of it. A fast ICME piles up the solar wind in front of it; when it catches up to an earlier ICME the leading shocks merge and strengthen. The resulting region of high-density, high-magnetic-field is called a merged interaction region, or MIR (see Burlaga, 1995). These structures have major effects on the heliosphere; since the magnetic field in these regions is large and variable, they slow the inward transport of energetic particles. Since MIRs have large pressures, they drive the termination shock outward a few AU (Zank and Muller, 2003). Most MIRs are observed at solar maximum and in the descending phase of the solar cycle. The large pressure pulses in the Voyager 2 data in Fig. 2 are MIRs. A few occurred from 1980 to 1985 at 10–20 AU, a few large ones were observed near the solar maximum in 1990 at about 30 AU, but beginning in 1999 the whole solar wind structure was dominated by a series of MIRs. The nature of the MIRs changed as well; at 65 AU the speed, density, pressure, and magnetic field magnitude were strongly correlated (Richardson et al., 2003). The MIRs recur roughly twice/year with pressure increases of a factor of 6–10. MIR formation and evolution were modeled using ACE data as input to a 1-D MHD model which includes pickup ions (Richardson et al., 2003). Fig. 3 compares the speed and density correlations predicted by the model with those observed by V2 as a function of distance. The model correlations increase with distance, showing that the density and speed variations become more and more in phase as the MIRs evolve. The observations and model agree only near solar maxima (the hatched regions). Since we use solar maximum data as input this result is not surprising; the MIRs form mainly under solar maximum conditions.

The morphology of shocks driven by ICMEs also changes over the solar cycle. At solar minimum fewer ICMEs occur, but those that do extend in latitude across the boundaries of the fast and slow solar wind. Thus the high-latitude parts of the

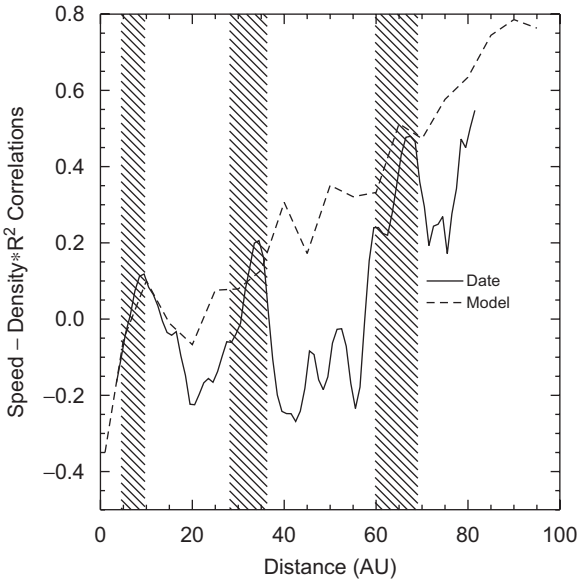

Fig. 3. Correlations between the speed and density. Solid line shows correlations of 25-day running averages of the Voyager 2 data; the correlations were done over 5 AU intervals of data, one point/AU. The dashed line shows the equivalent model values. The hashed regions indicate solar maxima.

ICME move faster, resulting in an ICME and shock with a concave shape. At solar maximum the solar wind speed is constant with latitude, so the ICME should have a convex shape (Liu et al., 2006). Fig. 4 shows the two configurations in the top panels. The shock orientations at solar maximum (left) and solar minimum (right) have been separated to look for this effect. The bottom panels of Fig. 4 show the shock normal elevation angles θ plotted versus heliolatitude δ at solar maximum (left) and solar minimum (right). These shock normals are determined from Ulysses data for solar maximum and from WIND and ACE data for solar minimum. The dashed lines show the angles expected for a convex shock with a radius of curvature of 1 AU. The circled points indicate slopes in the opposite direction to the rest of the shock normals. The dates of these anomalous points are given to show that they are at the edges of the solar minimum or maximum period. At solar minimum, the slope of the fit to the elevation angles is negative and the radius of curvature is -0.3 AU. Near solar maximum, the points fall very close to the line expected for a concave shock with a 1 AU radius of curvature. Thus the shock orientations change with solar cycle; these orientations may lead to more efficient particle acceleration at solar minimum.

The abundance of helium in the solar wind also varies over a solar cycle (Ogilvie and Hirshberg, 1974; Feldman et al., 1978). The lower abundances at solar minimum were attributed to the heliospheric current sheet (HCS) having a low He/H ratio. At solar minimum, the HCS is more often at low latitudes. At solar maximum, more fast wind and ICMEs are observed which have high He/H ratios. The solar wind He/H ratio has a strong linear dependence on the solar wind speed near solar minimum, but near solar maximum all solar wind speeds have a high He/H ratio (Aellig et al., 2001). Near solar minimum, the He/H ratio has a 6-month periodicity, with peaks when Earth is furthest from the heliospheric equator, suggesting the He/H ratio is a strong function of heliolatitude. These observations of the He/H ratio lead to the hypothesis that the slow solar wind has two separate sources, one near the HCS with low He/H abundance and another at higher heliolatitudes with a larger He/H abundance.

Fig. 5 shows histograms of the relative He/H abundance from wind for three times in the solar cycle, solar maximum (2000.3–2001), the ascending phase (1999.0–1999.6), and solar minimum (1996.2–1996.9). These data are all for slow solar wind, $v<400$ km/s, and for heliolatitudes of $\pm 7.25^{\circ}$. The solar minimum He/H profile shows a strong peak just below 1%, a small peak at 1.5%, and a tail up to 4%. The ascending phase He/H profile shows a peak at 1% and another at 3% with a significant tail extending beyond 6%. The solar maximum He/H profile has a broad peak between 3% and 4% and a large tail extending above 6%. But it also has a small peak at 1%. The HCS source seems to be always present with a He/H ratio of about 1%; at solar minimum, this region is the major source of solar wind at 1 AU. At solar maximum, the HCS is highly tilted so this source intersects Earth only a small percentage of the time. The rest of the solar wind is from ICMEs and/or a separate source of slow wind with a He/H ratio of 3–4%. Between solar minimum and solar maximum the ratio of the two sources varies as the HCS tilt angle changes.

3. Summary

Many aspects of the solar wind change over a solar cycle. The change in the solar configuration from the large latitudinal gradients seen near solar minimum to the small gradients near solar maximum leads to solar cycle variations in the correlation between solar wind parameters, the elevation

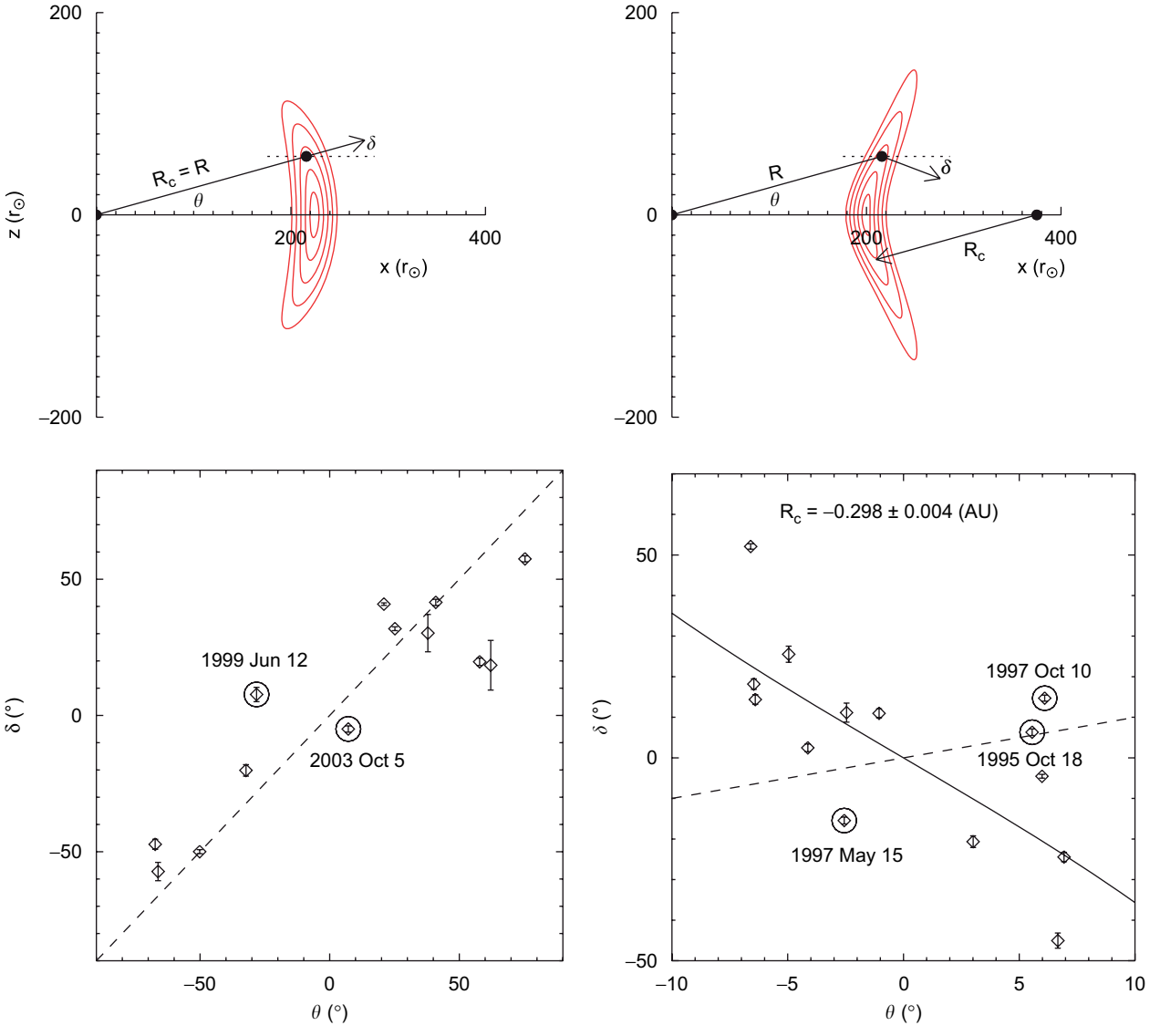

Fig. 4. Top panels show the ICME geometry in the GSE coordinate system expected at solar maximum (right) and solar minimum (left). The bottom panels show the shock normal angles θ plotted as a function of heliolatitude δ at solar maximum and solar minimum. The dashed lines show the shock normal angles expected for a radial shock. A radial shock fits the data well at solar maximum, but at solar minimum the best fit to the shock angles has the opposite slope consistent with the solar minimum geometry shown on the top right. Adapted from Liu et al. (2006).

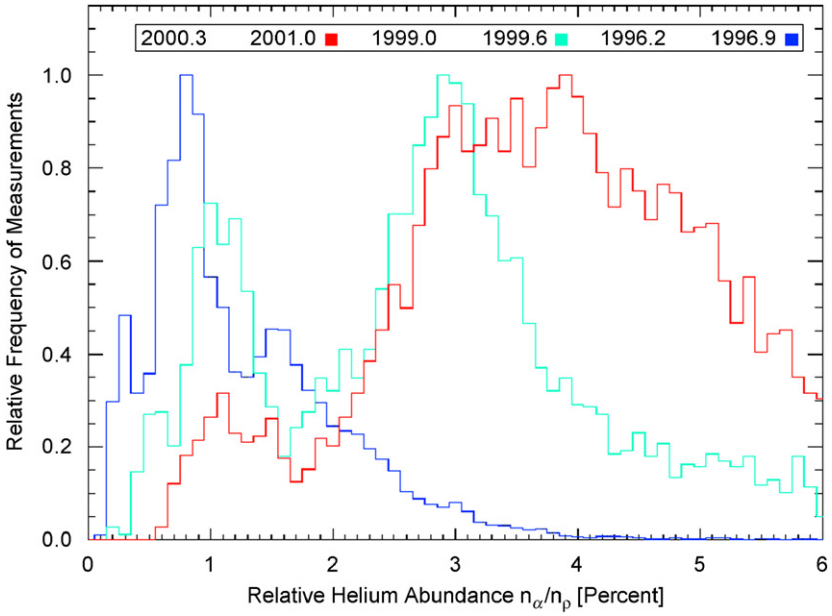

Fig. 5. Histograms of the He/H ratio in the solar wind at solar minimum (1996.2–1996.9), solar maximum (2000.3–2001), and the ascending phase of the solar cycle (1999.0–1999.6).

angle of shock normals, and the abundance of He/H observed at 1 AU. Some parameters change independent of heliolatitude, such as the solar wind dynamic pressure and the magnetic field magnitude. Some structures, such as MIRs, vary with distance as well as solar cycle, amplifying the solar cycle effects in the outer heliosphere. The diversity and distribution of solar cycle variations reaffirms the importance of having a global heliospheric monitoring system in place to monitor the solar surface and the solar wind at all heliolatitudes and all heliolongitudes.

Acknowledgments

This work was supported at M.I.T. under NASA contract 959203 from JPL to MIT, NASA Living with a Star TRT grant NNX06AC27G-44A081164, and NASA grant NAG-10915. This work was also supported in part by the International Collaboration Research Team Program of the Chinese Academy of Sciences.

References

Aellig, M.R., Lazarus, A.J., Steinberg, J.T., 2001. The solar wind helium abundance: variation with wind speed and the solar cycle. Geophysical Research Letters 28, 2767–2770.

Burlaga, L.F., 1995. Interplanetary Magnetohydrodynamics. Oxford University Press, New York.

Burlaga, L.F., Ness, N.F., Wang, Y.-M., Sheeley Jr., N.R., 2002. Heliospheric magnetic field strength and polarity from 1 to 81 AU during the ascending phase of solar cycle 23. Journal of Geophysical Research 107 (A11), 1410.

Cane, H.V., Richardson, I.G., 2003. Interplanetary coronal mass ejections in the near-Earth solar wind 1996–2002. Journal of Geophysical Research 108, 1156.

Feldman, W.C., Asbridge, J.R., Bame, S.J., Gosling, J.T., 1978. Long-term variations of selected solar wind properties: IMP 6, 7, and 8 results. Journal of Geophysical Research 83, 2177.

Gazis, P.R., 1996. Solar cycle variation in the heliosphere. Reviews of Geophysics 34 (3), 379–402.

Gosling, J.T., McComas, D.J., Phillips, J.L., Bame, S.J., 1992. Counterstreaming solar wind halo electron events: solar cycle variations. Journal of Geophysical Research 97, 6531–6535.

Gringauz, K.I., 1961. Some results of experiments in interplanetary space by means of charged particle traps on Soviet space probes. Space Research 2, 539–553.

Liu, Y., Richardson, J.D., Belcher, J.W., Wang, C., Hu, Q., Kasper, J.C., 2006. Constraints on the global structure of magnetic clouds: transverse size and curvature. Journal of Geophysical Research 111, A12S03.

McComas, D.J., Gosling, J.T., Skoug, R.M., 2000. Ulysses observations of the irregularly structured mid-latitude solar wind during the approach to solar maximum. Geophysical Research Letters 27, 2487.

Neugebauer, M., 1975. Large scale solar cycle variations of the solar wind. Space Science Reviews 17, 221.

Neugebauer, M., Snyder, C.W., 1966. Mariner 2 observations of the solar wind, 1, average properties. Journal of Geophysical Research 71, 4469.

Ogilvie, K.W., Hirshberg, J., 1974. The solar cycle variation of the solar wind helium abundance. Journal of Geophysical Research 79, 4959.

Richardson, J., Wang, C., 1999. The global nature of solar cycle variations of the solar wind dynamic pressure. Geophysical Research Letters 26, 561–564.

Richardson, J.D., Wang, C., Burlaga, L.F., 2003. Correlated solar wind speed, density, and magnetic field changes at Voyager 2. Geophysical Research Letters 30 (23), 2207.

Richardson, J.D., Liu, Y., Wang, C., Burlaga, L.F., 2006. ICMEs at very large distances. Advances in Space Research 38, 528–534.

Zank, G.P., Muller, H.-R., 2003. The dynamical heliosphere. Journal of Geophysical Research 108, 1240.